Accepted Manuscript

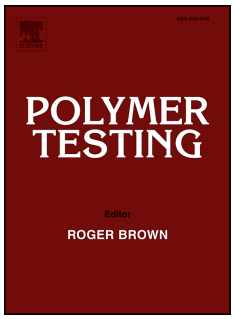

Investigation of bulk and *in situ* mechanical properties of coupling agents treated wood plastic composites

Yonghui Zhou, Mizi Fan, Lanying Lin

PII: S0142-9418(16)31171-0

DOI: 10.1016/j.polymertesting.2016.12.026

Reference: POTE 4879

To appear in: *Polymer Testing*

Received Date: 28 October 2016

Accepted Date: 21 December 2016

Please cite this article as: Y. Zhou, M. Fan, L. Lin, Investigation of bulk and *in situ* mechanical properties of coupling agents treated wood plastic composites, *Polymer Testing* (2017), doi: 10.1016/j.polymertesting.2016.12.026.

Investigation of bulk and *in situ* mechanical properties of coupling agents treated wood plastic composites

Yonghui Zhou, Mizi Fan*, Lanying Lin

Department of Civil Engineering, College of Engineering, Design and Physical Sciences, Brunel University London, UB8 3PH, United Kingdom

Abstract: This paper presents the interfacial optimisation and characterisation of WPC by the use of maleated and silane coupling agents (MAPE, Si69 and VTMS), and its effect on the bulk and *in situ* mechanical properties. The results showed the treated WPC possessed better interface by showing improved compatibility between the constituents, wettability of wood flour, and resin penetration in the SEM images. The enhanced interface led to the increase in the tensile strength and stiffness of the treated WPC, which was confirmed by their superior load bearing capacity, namely the higher storage moduli measured by DMA. The observed shift of the relaxation peak of the treated WPC indicated the constraints on the segmental mobility of the polymeric molecules resulted from the treatments. Nanoindentation investigation revealed that the *in situ* mechanical properties were subject to a number of phenomena including fibre weakening or softening impact, crystalline structure transformation and cell wall deformation, concluding that the bulk mechanical properties of WPC might not be governed by the local property of materials within the interface.

Key words: wood plastic composites; bulk property; interface structure; interfacial property; nanoindentation

1 Introduction

Wood plastic composites (WPC) has recently experienced considerable expansion, mainly because of the advantageous features that wood material possesses, namely ubiquitous availability at low cost and in a variety of forms, renewability and biodegradability, low

* Corresponding author. Tel.: +44 7790390554; Fax: +44 1895 256392
Email address: fanfafu@gmail.com

density, nontoxicity, flexibility during processing, and acceptable specific strength properties [1-7]. However, the formulation of WPC was perturbed by the inherently polar and hydrophilic nature of wood flour or fibre, which makes it least compatible with hydrophobic polymeric matrices. The poor combination of wood and polymer is not able to generate the designed performance [4, 8]. To avoid these drawbacks, various specific structural modifications approaches have been studied, such as corona treatment, plasma treatment, UV and gamma radiation treatments, surface compatibilisation and copolymerisation [8, 9].

The performance and behaviour of WPC was not only relying on the reinforcing wood and the polymer matrix, but also critically depending on the effectiveness of load/stress transfer across the interface [10, 11]. The interface of WPC formed when the wood flour is embedded in the polymer matrix during fabrication of the composite is a heterogeneous transition zone with distinct chemical compositions, morphological features and mechanical properties from those of the reinforcing phase and the bulk polymer [11-13]. An appropriately engineered interface could considerably improve the strength and toughness of the composite as well as the environmental stability. Therefore, on the other hand, the determination of interfacial properties and characteristics would be of utmost importance in evaluating the overall property of the composite and enabling its optimal design [14]. Numerous techniques, such as single fibre fragmentation test, single fibre pull-out test and microbond test, have been developed for characterising the fibre/matrix interfacial strength. However, very few studies have carried out the determination of the size and relative mechanical properties of the interface due to the lack of unequivocally established experimental techniques.

Nanoindentation technique has been proven to be an effective method in determining material surface properties at nanoscale, which is achieved by monitoring a probe penetrating into the specimen surface and synchronously recording the penetration load and depth [15, 16]. It has recently found its application feasible to wood, natural fibres and plastics [12, 15, 17-24], but it has been rarely employed in measuring the interface property and performance of WPC materials. A study on the effect of water absorption on the nanomechanical properties of woven fabric flax fibre-reinforced bioresin-based epoxy biocomposites observed approximately 35% and 12% deductions of nanohardness and reduced modulus respectively, after exposure to water, indicating that the strength and

elastic modulus were fibre-sensitive properties in the composites and the interface suffered from the water absorption [25]. Nanoindentation was also conducted to measure the hardness and elastic modulus of in the interface region of cellulose fibre-reinforced PP composite. There was a gradient of hardness and modulus across the interface region, and the distinct properties were revealed by 1-4 indents depending on the nanoindentation depth and spacing [12].

The incorporation of silane and maleated coupling agents exerted reinforcing impact on the global property of WPC materials, but its influence on the mechanical properties in the interface region has not yet been reported in the literatures. In this work, WPC materials were fabricated by the use of recycled wood flour and PE aiming at reducing the consumption of virgin raw materials and the environmental impact. The focus of this work was to optimise the interface of WPC by incorporating three different coupling agents, i.e. maleic anhydride grated polyethylene (MAPE), bis(triethoxysilylpropyl)tetrasulfide (Si69) and vinyltrimethoxysilane (VTMS); hence to reveal the interface structure and bonding scenarios of the formulated WPC. More importantly, the influence of the coupling agent treatments on the *in situ* mechanical properties of coupling agent treated WPC was first determined by carrying out nanoindentation analysis, which led to thorough understanding of interfacial characteristics and the correlation between *in situ* and bulk mechanical properties.

2 Materials and methods

2.1 Materials

Recycled wood flour used in this work was supplied by Rettenmeier Holding AG (Germany), with a bulk density of 0.285 kg/m^3; recycled polyethylene (PE) pellet with a bulk density of 0.96 kg/m^3 and MFI of 0.6g/10min at 190^{o}C was obtained from JFC Plastics Ltd (UK); lubricants 12-HSA (12-Hydroxyoctadecanoic acid) and Struktol TPW 709 were purchased from Safic Alcan UK Ltd (Warrington, UK); coupling agents, MAPE (500cP viscosity at 140^{o}C, 0.5 wt% of maleic anhydride), Si69 (> 95% purity, 250^{o}C boiling point) and VTMS (> 98% purity, 123^{o}C boiling point), were purchased from Sigma-Aldrich (Dorset, UK), and their chemical formulae were presented in Fig. 1. All the raw materials and additives were stored in a cool and dry place before uses.

2.2 Formulation of composites

The formulation of untreated and treated WPC with specific ratios was summarised in Table 1. All the composites were carefully prepared under the same processing condition as follows: the required amount of PE for each batch was firstly placed in a Brabender Plastograph twin-screw mixer and allowed to melt at 100 rpm and 190 ^{o}C for 2 min, and subsequently mixed with wood flour for 3 min. The lubricants and/or coupling agents were thus added into system and mixed for another 10 min. The resulted mixture was thus ground to pellets by using a Retsch cutting mill (SM 100, Germany). The ground blends were compression moulded on an electrically heated hydraulic press. Hot-press procedures involved 20 min preheating at 190 ^{o}C with no load applied followed by 10 min compressing at the same temperature under the pressure of 9.81 MPa, and subsequently air cooling under load until the mould reached 40 ^{o}C.

2.3 Characterisation of WPC microstructure

All the composites were transversely cut by using a sliding microtome with the nominal thickness of around 25 microns for the morphological investigation of the cross sections. The observation was conducted on a Leo 1430VP Scanning Electron Microscope (SEM) operating at 10 kV, all the samples were conductively plated with gold by sputtering for 45 s before imaging.

2.4 Tensile property analysis

Tensile properties of the composites were determined at a crosshead speed of 1 mm/min according to the standard BS EN ISO 527-2:2012 on an Instron 5900 testing machine with 30 kN load capacity. For each sample, the tensile property reported is the average of six measurements. The tensile properties of recycled PE were also measured and given for reference: tensile stress at maximum load 23.05±0.17 MPa, tensile strain at maximum load 10.35±0.32%, tensile modulus 2385.41±133.25 MPa.

2.5 Dynamic mechanical analysis (DMA)

Dynamic mechanical properties of the composites were measured by using a dynamic mechanical analyser (Q800, TA Instruments, New Castle, USA) under single cantilever strain-controlled mode. The temperature ranges from -100^{o}C to 120^{o}C with a heating rate of 3

^{o}C/min. The oscillation amplitude was 20 μm, the frequency was 1 Hz, and the specimen dimension was 17.5 mm × 10.8 mm × 1.4 mm.

2.6 Nanoindentation analysis

The samples for nanoindentation determination were prepared as follows: a sloping apex (around 45^{o}) was created on the cross section of the sample by using a sliding microtome, thus the sample was mounted onto an ultramicrotome (Leica EM UC7, Germany) and transversely cut with a glass knife and a diamond knife to obtain an exceptionally smooth and flat surface. The cross section of the samples was firstly observed under an optical microscope to select the regions to be indented (Fig. 2a). The tests were performed on a Nano Indenter (Hysitron TI 950 TriboIndenter, USA) equipped with a three-side pyramid diamond indenter tip (Berkovich). In each test region, the space between two adjacent testing positions was more than 30 times of the maximum indentation depth (Fig. 2b-2c). The indentations were conducted under load-controlled mode consisting of three segments, i.e. loading with 150 μN in 5 seconds, holding for 2 seconds, and unloading in 5 seconds. A typical loading-displacement curve was presented in Fig. 3. The maximum load P_{max}, the maximum depth h_{max}, the final depth after unloading h_r, and the slope of the upper portion of the unloading curve S were monitored in a full loading-unloading cycle. The material properties, such as reduced elastic modulus and hardness, could be extracted by analysing these data with the method developed by Oliver and Pharr [20].

The hardness (H) was calculated as follows:

$$H = \frac{P_{max}}{A} \quad \text{Eq. 1}$$

Where, A is the projected contact area at maximum load. Er, the reduced elastic modulus accounting for the compliance of the indenter tip, was determined as:

$$E_r = \frac{\sqrt{\pi}}{2}\frac{dP}{dh}\frac{1}{\sqrt{A}} \quad \text{Eq. 2}$$

Where, $dp/dh = S$. The results reported in the work were from the indentations placed in the valid positions, namely clearly on the cells with intimate and firm resin contact, excluding the results from cracks and other positions.

3 Results and discussions

3.1 Interfacial structure analysis

The interface region formed between wood flour and matrix is in fact a zone of compositional, structural and property gradients, generally varying in width from a single atom layer to micrometers. The effect of the coupling agent treatments on the interfacial structure of the composites was shown in Fig. 4. It can be seen that a number of clear cracks or boundaries between wood particles and the matrix occurred in the untreated WPC (Fig.4a), which indicated an inferior compatibility between the untreated raw materials. It was also observed that there were a few cell lumens partially filled by the polymer resin. However, the majorly unfilled cell lumens along with the existence of micro cracks between wood and PE indicated the poor interfacial adhesion of the untreated WPC. By contrast, the wood flour in the treated samples was completely coated by the matrix and firmly bonded to polymer resin (Fig.4b-4d), demonstrating superior interfacial adhesion with resin impregnation throughout the interface. More importantly, a large number of cell lumens of these samples were discerned to be partially or utterly filled by the polymer which again confirmed the enhanced interfacial adhesion and also compatibility and wettability.

It was interesting that apart from the cell lumens, the vessels of the wood particles in the treated samples, especially the VTMS treated sample, were also completely or partially impregnated with PE polymer. This phenomenon may be related to the substantially deformed and damaged cell lumens and vessels (Fig.4d), which were inclined to facilitate the flow of the polymer in the composite. Hydrodynamic flow of molten PE resin in the composites may be initiated by an external compression force through vessels, and then proceed into the interconnected network of cell lumens and pits in interface region, with flow moving primarily in the paths of least resistance [26, 27]. The flow paths in any directions were in general a combination of open cut lumens and vessels as well as of large pits.

3.2 Bulk mechanical properties

3.2.1 Tensile properties

The effect of incorporation of coupling agents on the tensile properties of WPC was summarised in Table 2. The application of MAPE, Si69 and VTMS led to a significant increase in the tensile strength of the composites by 135.40%, 15.63%, and 77.40% respectively. The

treated WPC also demonstrated much greater tensile moduli than the untreated one (112.73%, 63.3%, and 114.15% respectively), indicating the notable enhancement of the stiffness of the composites. Similar results had been observed in the study of maleic anhydride polypropylene (MAPP) treated wood flour/recycled PE composites and VTMS treated wood flour/PE composites: the addition of 3% MAPP led to the increase of the tensile strength (48.78%) and Young's modulus (MOE, 28.24%) of wood flour/recycled PE (50%/47%) composite [28]; the incorporation of VTMS (0.5%-2%) improved the tensile strength and tensile modulus of wood flour/PE composites by up to 62% and 14% respectively [29]. These phenomena were evidently resulted from the enhanced physical, chemical and mechanical bonding of the interface between wood flour and the matrix with the addition of the coupling agents, which was thoroughly discussed in our previous study [30], namely the chemical reactions occurred between the intrinsically multifunctional coupling agents and the constituents of the composites (i.e. the hydrophilic moieties including maleic anhydride groups of MAPE, ethoxy groups of Si69 and methoxyl groups of VTMS covalently bonded with the hydroxyl groups of wood flour, while the hydrophobic PE chains in MAPE, sulfide groups in Si69 and vinyl groups in VTMS crosslinked with the PE macromolecules), the increased interdiffusion between the substrates due to the better chemical compatibility resulted from the chemical reactions, the enhanced wettability of wood flour by the resin, as well as the more resin penetration and impregnation and mechanical interlocking at the interface.

In addition, according to the classic mechanics theory of particle-reinforced material [31], the load applied to WPC was transferred from PE matrix to wood flour by shear stress along the interface. The presence of the coupling agents in WPC promoted the dispersion and distribution of wood flour in the matrix, resulting in better interfacial adhesion and more efficient stress transfer from the matrix to wood flour, thus the improvement of the mechanical properties. The tensile strain of the treated WPC was also decreased by 24.58% (MAPE), 55.93% (Si69), and 59.32% (VTMS). This also reflected more compact and stiffer structure of the WPC. Furthermore, it was worth mentioning that although the standard deviation of the tensile strain results (5%-10%) was not as low as those of tensile stress and modulus (around or less than 5%), it did not appear to be affecting the investigation of the variation of the tensile properties of the composites.

3.2.2 Dynamic mechanical analysis (DMA)

Storage modulus is closely related to the load bearing capacity of a material [32, 33]. The variation of storage modulus of WPC as a function of temperature was graphically enumerated in Fig. 5. It was observed that similar to the tensile modulus, the coupling agents MAPE and VTMS treated WPC gave much higher storage moduli than the untreated one, primarily attributing to the improved interfacial adhesion between wood flour and the matrix. The storage moduli in all composites decreased with the increase of temperature, and the differentiation of the modulus between the treated and untreated WPC gradually diminished from the transition region (-100 – 75^{o}C) to plateau region (75 – 120^{o}C).

The loss modulus-temperature curves in Fig. 5 were used to investigate the transition behaviour of the composites. There was one major transition (45 – 60^{o}C) existed in these curves corresponding to the α transition of PE matrix, which was associated with the chain segment mobility in the crystalline phase due to the reorientation of defect area in the crystals [7, 32, 33]. In comparison to the relaxation peak of untreated WPC (47.93^{o}C), the counterparts of MAPE and VTMS treated WPC had shifted towards higher temperature regions (i.e. 57.35^{o}C and 51.79^{o}C for MAPE and VTMS respectively), and the corresponding moduli of the treated WPC (i.e. 232.40 MPa and 201.93 MPa for MAPE and VTMS respectively) were accordingly higher than that of the untreated one (181.43 MPa). These performance should be attributed to the generated constraints on the segmental mobility of polymeric molecules at the relaxation temperatures during the coupling agent treatments [31, 34].

It was worth noticing that compared to the untreated WPC, albeit the α transition appeared at higher temperature (52.94^{o}C) Si69 treated composite showed a reduced loss modulus (166.72 MPa), indicating that Si69 treatment did not lead to comparable segmental immobilisation of the matrix chains on the wood surface as MAPE and VTMS treatments. This might be related to the comparatively limited crosslinking between the polysulfides of Si69 and PE molecules compared to that between the grafted PE on MAPE or the unsaturated C=C groups of VTMS and the PE matrix molecules (the chemical formulae of coupling agents were shown in Fig.1), which was in agreement with the less evident discrimination of the corresponding spectral characteristics in its chemical structure analysis, especially the FTIR (Fourier Transform Infrared spectroscopy) analysis in our previous study

[30]. Similarly, the tensile strength and modulus of Si69 treated WPC were inferior to those of MAPE and VTMS treated composites. However, it had been reported that transition peak broadens and the peak position shifts if there is an interaction between the filler or reinforcement and matrix polymer [35]. Therefore, the broadening of the transition regions from around 10^{o}C to 85^{o}C discerned in all the treated composites (especially MAPE and VTMS treated composites) might be an indication of the existence of the interaction between the coupling agents and the constituents of the composites.

The ratio of the loss modulus to storage modulus defining as damping factor tanδ was also determined (Fig. 5) for the benefits of better understanding the damping behaviour and interface property of the composites. As can be seen in Fig. 5, the tanδ amplitude of the composites decreased with the addition of the coupling agents. This was expected since the enhanced interfacial adhesion provided the treated WPC with an interface of higher stiffness which in turn restrained the segmental mobility of polymer molecules leading to the decrease of tanδ magnitude [31, 34, 35]. In addition, the composite with poorer interfacial bonding between wood flour and matrix was inclined to dissipate more energy, showing greater tanδ amplitude than the composite with firmly bonded interface [31, 36, 37].

Adhesion factor, A, was thus determined from the mechanical damping (tanδ) to further investigate the effect of the coupling agent treatments on the interfacial adhesion between the filler and matrix of the composites in accordance with the following equation reported by Correra [38] and Kubat [39]:

$$A = \frac{tan\delta_c}{(1-V_w)tan\delta_m} - 1 \qquad \text{Eq. 3}$$

Where, the subscripts c, m and w refer to composite, matrix, and wood flour respectively, and V_w is the volume fraction of wood flour in the composite. As Fig. 6 showed, the untreated composite had higher adhesion factor than the coupling agent treated composites, which was consistent with the tanδ results. According to Correra [38], the molecular mobility of the polymer surrounding the filler was reduced at high levels of interfacial adhesion, and consequently low values of the adhesion factor suggested improved interactions at the filler-matrix interface. The determined lower levels of adhesion factor in coupling agent treated WPC evidently confirmed the enhanced interfacial

interactions after the treatments, which resulted in the decreased molecular mobility and mechanical damping (tanδ) [39-41]. In addition, the adhesion factor of Si69 treated composite was higher than those of MAPE and VTMS treated composites. This result along with its relatively greater tanδ amplitude again substantiated the inferior interfacial adhesion improvement induced by Si69 treatment, resulting in the comparatively lower tensile strength, tensile modulus, storage modulus and loss modulus of the composite determined in the above sections.

3.3 In situ mechanical properties

The examination of the mechanical properties at nanoscale would undeniably help reveal the interface characteristics and evaluate the overall property of the composites. Fig. 7 demonstrated the nanomechanical properties of the wood cell walls of the composites determined by nanoindentation. It is most interesting that the untreated composite showed an elastic modulus of 16.42 GPa and a hardness of 0.53 GPa, while the counterparts of the MAPE and Si69 treated composites interestingly decreased to 11.46 GPa and 0.46 GPa (MAPE treated), and 15.60 GPa and 0.49 GPa (Si69 treated) respectively. This is in disagreement with that of the bulk properties tested. The drops of the modulus and hardness were assumed to be partially resulted from the fibre weakening or softening impact of the treatments, namely the chain scission (cleavage of β-1,4-glycosidic bonds between two anhydroglucose units) and weakening of interfibrillar interaction in cellulose occurred with the presence of maleic and silane coupling agents under high pressure and temperature during processing [42, 43]. On the other hand, it might be associated with the degree of crystalline orientation in wood flour. NMR (Nuclear Magnetic Resonance spectroscopy) results of the composites (not shown in the work) indicated that the crystalline carbohydrates in wood flour underwent transformation into an amorphous form during the treatments, which might facilitate the nanoindentation loading along the fibre direction, and thus, lower modulus and hardness were measured. Although the VTMS treatment had the analogous effects on the composites, there was no noticeable difference between the untreated and VTMS treated composites, in terms of their elastic modulus and hardness. This suggested that there were other critical factors governing the *in situ* mechanical properties of the composites. Due to the relatively lower molecular weight (M_W) of Si69 (M_W=539) and VTMS (M_W=148) than MAPE (500 cps viscosity at 140^{o}C), silanes might

be more capable of diffusing into cell walls and reacting with the structural components by forming hydrogen and covalent bonding, giving rise to more outstanding nanomechanical property. In addition, the maleic coupling agent was found to be able to create a thin, soft and ductile interfacial layer in the composite [44], which might impart an adverse impact on the nanomechanical property of the composite. More importantly, the better nanaomechanical property of VTMS treated composite over MAPE and Si69 treated composites should be ascribed to the severe deformation and damaging of its cell walls due probably to the compression under high pressure and temperature. The SEM analysis had shown that VTMS treated composite possessed much more deformed and damaged cell lumens and vessels than the untreated and MAPE and Si69 treated composites, which promoted the wetting of wood flour by the polymer and the polymer penetration into wood particles. The higher level of penetration was assumed to compensate the loss of the *in situ* mechanical properties due to the aforementioned fibre weakening or softening impact and crystalline structure transformation. Therefore, the nanomechanical property of the treated composites fell into the sequence: VTMS > Si69 > MAPE.

It should be pointed out that the employed coupling agent treatments enhanced the interfacial adhesion and bonding of the composites by strengthening the chemical, physical, and mechanical bonding (i.e. interdiffusion, electrostatic adhesion, chemical reaction and mechanical interlocking), which had been substantiated by a set of investigation including FTIR, NMR, FM (Fluorescence Microscope), and SEM analyses in our previous work [30]. The optimised interface contributed to the increase of the bulk mechanical properties of the composites. Although both the MAPE and VTMS treated composites demonstrated significant increase of bulk mechanical properties (i.e. tensile stress (Table 2), storage and loss modulus (Fig. 5)) after the treatments, the corresponding *in situ* mechanical properties were different; MAPE treated composite possessed a softer interface by showing lower *in situ* elastic modulus and hardness than the VTMS treated. In comparison to that of VTMS treated composite, the comparatively softer and tougher interface of MAPE treated might provide it with greater resistance to fracture, which accounted for the higher tensile strain (85.42%, Table 2). In addition, owing to the inherently tough and ductile nature of PE matrix, the softer and tougher interface might benefit the continuity in load transfer from the

matrix to wood flour, promoting the composite to function as a mechanical entity, thus leading to higher tensile strength.

It was evident that to what extent the bulk mechanical properties of the composite could be improved was predominantly relying on the level of the enhancement of compatibility, interfacial adhesion and bonding after different coupling agent treatments rather than individual local property within the interface. The distinct nature and characteristics of the interfaces might play another fundamental role in determining the global properties of the composites.

4 Conclusions

The influence of the incorporation of MAPE, Si69 and VTMS coupling agents on the interfacial structure, bulk and *in situ* mechanical properties of WPC has been examined. SEM observation revealed that the coupling agent treatments enhanced the interfacial compatibility and adhesion of WPC by promoting the wood flour dispersion in the matrix, improving the wettability of wood flour by the resin, and facilitating the resin impregnation throughout the interface. The better interfacial adhesion and more efficient stress transfer from the matrix to wood flour led to the improvement of the tensile strength, tensile modulus and storage modulus of the treated WPC, while the tensile strain of the composites suffered from the stiffen impact of the treatments. The coupling agent treatments restrained the segmental mobility of polymer molecules of the matrix, resulted in the shift of relaxation peak and the diminutions of tanδ magnitude. The relatively lower level of adhesion factor confirmed the enhanced interfacial interactions in the treated composites. The decreased (MAPE and Si69 treated) and unaffected (VTMS treated) nanomechanical properties of the treated WPC determined by nanoindentation suggested that the *in situ* mechanical properties were not primarily governed by the interfacial adhesion, but more significantly affected by fibre weakening or softening impact, crystalline structure transformation and cell wall deformation/damaging. In other words, the bulk property of WPC was not governed by the individual local property of materials within the interface.

5 Acknowledgements

The authors gratefully acknowledge the financial support from the European CIP-EIP-Eco-innovation-2012 (Project Number: 333083).

6 References

1. H. Zhang. Effect of a novel coupling agent, alkyl ketene dimer, on the mechanical properties of wood–plastic composites. Mater Des 2014;59:130-134.

2. P. Kuo, S. Wang, J. Chen, H. Hsueh, M. Tsai. Effects of material compositions on the mechanical properties of wood–plastic composites manufactured by injection molding. Mater Des 2009;30(9):3489-3496.

3. Y. Xie, C.A.S. Hill, Z. Xiao, H. Militz, C. Mai. Silane coupling agents used for natural fiber/polymer composites: A review. Composites Part A 2010;41(7):806-819.

4. M.N. Belgacem, A. Gandini. The surface modification of cellulose fibres for use as reinforcing elements in composite materials. Composite Interfaces 2005;12(1-2):41-75.

5. M. Bengtsson, N.M. Stark, K. Oksman. Durability and mechanical properties of silane cross-linked wood thermoplastic composites. Composites Sci Technol 2007;67(13):2728-2738.

6. M. Bengtsson, K. Oksman. The use of silane technology in crosslinking polyethylene/wood flour composites. Composites Part A: Applied Science and Manufacturing 2006;37(5):752-765.

7. M. Bengtsson, P. Gatenholm, K. Oksman. The effect of crosslinking on the properties of polyethylene/wood flour composites. Composites Sci Technol 2005;65(10):1468-1479.

8. M.J. Spear, A. Eder, M. Carus. 10 - Wood polymer composites. Woodhead Publishing. 2015.

9. R. Malkapuram, V. Kumar, Yuvraj Singh Negi. Recent Development in Natural Fiber Reinforced Polypropylene Composites. Journal of Reinforced Plastics and Composites 2009;28(10):1169-1189.

10. R. Kumar, W.M. Cross, L. Kjerengtroen, J.J. Kellar. Fiber bias in nanoindentation of polymer matrix composites. Composite Interfaces 2004;11(5-6):431-440.

11. T.D. Downing, R. Kumar, W.M. Cross, L. Kjerengtroen, J.J. Kellar. Determining the interphase thickness and properties in polymer matrix composites using phase imaging atomic force microscopy and nanoindentation. J Adhes Sci Technol 2000;14(14):1801-1812.

12. S. Lee, S. Wang, G.M. Pharr, H. Xu. Evaluation of interphase properties in a cellulose fiber-reinforced polypropylene composite by nanoindentation and finite element analysis. Composites Part A 2007;38(6):1517-1524.

13. J. Kim, Y.W. Mai. Engineered interfaces in fiber reinforced composites. Elsevier Sciences. 1998.

14. J.F. Graham, C. McCague, O.L. Warren, P.R. Norton. Spatially resolved nanomechanical properties of Kevlar® fibers. Polymer 2000;41(12):4761-4764.

15. T. Zhang, S.L. Bai, Y.F. Zhang, B. Thibaut. Viscoelastic properties of wood materials characterized by nanoindentation experiments. Wood Sci Technol 2012;46(5):1003-1016.

16. G.L. Oliveira, C.A. Costa, S.C.S. Teixeira, M.F. Costa. The use of nano- and micro-instrumented indentation tests to evaluate viscoelastic behavior of poly(vinylidene fluoride) (PVDF). Polym Test 2014;34:10-16.

17. W. Gindl, J. Konnerth, T. Schöberl. Nanoindentation of regenerated cellulose fibres. Cellulose 2006;13(1):1-7.

18. M. Zare Ghomsheh, F. Spieckermann, G. Polt, H. Wilhelm, M. Zehetbauer. Analysis of strain bursts during nanoindentation creep of high-density polyethylene. Polym Int 2015;64(11):1537-1543.

19. J. Lee, Y. Deng. Nanoindentation study of individual cellulose nanowhisker-reinforced PVA electrospun fiber. Polymer Bulletin 2013;70(4):1205-1219.

20. W.C. Oliver, G.M. Pharr. An improved technique for determining hardness and elastic modulus using load and displacement sensing indentation experiments. J Mater Res 1992;7(6):1564-1583.

21. W.T.Y. Tze, S. Wang, T.G. Rials, G.M. Pharr, S.S. Kelley. Nanoindentation of wood cell walls: Continuous stiffness and hardness measurements. Composites Part A 2007;38(3):945-953.

22. J.K. Hobbs, A.K. Winkel, T.J. McMaster, A.D.L. Humphris, A.A. Baker, S. Blakely, M. Aissaoui, M.J. Miles. Nanoindentation of polymers: An overview. Macromolecular Symposia 2001;167(1):15-43.

23. Y. Wu, S. Wang, D. Zhou, C. Xing, Y. Zhang, Z. Cai. Evaluation of elastic modulus and hardness of crop stalks cell walls by nano-indentation. Bioresour Technol 2010;101(8):2867-2871.

24. C. Xing, S. Wang, G.M. Pharr. Nanoindentation of juvenile and mature loblolly pine (Pinus taeda L.) wood fibers as affected by thermomechanical refining pressure. Wood Sci Technol 2009;43(7-8):615-625.

25. H. Dhakal, Z. Zhang, N. Bennett, A. Lopez-Arraiza, F. Vallejo. Effects of water immersion ageing on the mechanical properties of flax and jute fibre biocomposites evaluated by nanoindentation and flexural testing. J Composite Mater 2014;48(11):1399-1406.

26. I.G. Grmusa, M. Dunky, J. Miljkovic, M.D. Momcilovic. Influence of the degree of condensation of urea-formaldehyde adhesives on the tangential penetration into beech and fir and on the shear strength of the adhesive joints. European Journal of Wood and Wood Products 2012;70(5):655-665.

27. I.G. Grmusa, M. Dunky, J. Miljkovic, M.D. Momcilovic. Influence of the viscosity of UF resins on the radial and tangential penetration into poplar wood and on the shear strength of adhesive joints. Holzforschung 2012;66(7):849-856.

28. K.B. Adhikary, S. Pang, M.P. Staiger. Dimensional stability and mechanical behaviour of wood–plastic composites based on recycled and virgin high-density polyethylene (HDPE). Composites Part B: Engineering 2008;39(5):807-815.

29. C.M. Clemons, R.C. Sabo, K.C. Hirth. The effects of different silane crosslinking approaches on composites of polyethylene blends and wood flour. J Appl Polym Sci 2011;120(4):2292-2303.

30. Y. Zhou, M. Fan, L. Lin. Revealing the interface structure and bonding mechanism of coupling agent treated WPC. Under review.

31. R. Ou, Y. Xie, M.P. Wolcott, S. Sui, Q. Wang. Morphology, mechanical properties, and dimensional stability of wood particle/high density polyethylene composites: Effect of removal of wood cell wall composition. Mater Des 2014;58:339-345.

32. S. Mohanty, S.K. Verma, S.K. Nayak. Dynamic mechanical and thermal properties of MAPE treated jute/HDPE composites. Composites Sci Technol 2006;66(3–4):538-547.

33. S. Mohanty, S.K. Nayak. Interfacial, dynamic mechanical, and thermal fiber reinforced behavior of MAPE treated sisal fiber reinforced HDPE composites. J Appl Polym Sci 2006;102(4):3306-3315.

34. M.A. López-Manchado, J. Biagitti, J.M. Kenny. Comparative study of the effects of different fibers on the processing and properties of ternary composites based on PP-EPDM blends. Polymer Composites 2002;23(5):779-789.

35. S. Lai, F. Yeh, Y. Wang, H. Chan, H. Shen. Comparative study of maleated polyolefins as compatibilizers for polyethylene/wood flour composites. J Appl Polym Sci 2003;87(3):487-496.

36. J.M. Felix, P. Gatenholm. The nature of adhesion in composites of modified cellulose fibers and polypropylene. J Appl Polym Sci 1991;42(3):609-620.

37. M. Ashida, T. Noguchi, S. Mashimo. Dynamic moduli for short fiber-CR composites. J Appl Polym Sci 1984;29(2):661-670.

38. C.A. Correa, C.A. Razzino, E. Hage. Role of Maleated Coupling Agents on the Interface Adhesion of Polypropylene—Wood Composites. Journal of Thermoplastic Composite Materials 2007;20(3):323-339.

39. J. Kubát, M. Rigdahl, M. Welander. Characterization of interfacial interactions in high density polyethylene filled with glass spheres using dynamic-mechanical analysis. J Appl Polym Sci 1990;39(7):1527-1539.

40. M. Poletto, M. Zeni, A.J. Zattera. Dynamic mechanical analysis of recycled polystyrene composites reinforced with wood flour. J Appl Polym Sci 2012;125(2):935-942.

41. H.L. Ornaghi, A.S. Bolner, R. Fiorio, A.J. Zattera, S.C. Amico. Mechanical and dynamic mechanical analysis of hybrid composites molded by resin transfer molding. J Appl Polym Sci 2010;118(2):887-896.

42. M.A. Sawpan, K.L. Pickering, A. Fernyhough. Effect of various chemical treatments on the fibre structure and tensile properties of industrial hemp fibres. Composites Part A: Applied Science and Manufacturing 2011;42(8):888-895.

43. C. Ganser, U. Hirn, S. Rohm, R. Schennach, C. Teichert. AFM nanoindentation of pulp fibers and thin cellulose films at varying relative humidity. Holzforschung 2013;68(1):53-60.

44. V. Hristov, S. Vasileva. Dynamic Mechanical and Thermal Properties of Modified Poly(propylene) Wood Fiber Composites. Macromolecular Materials and Engineering 2003;288(10):798-806.

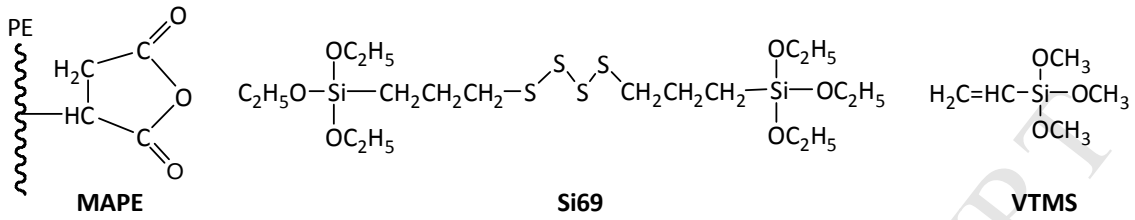

Fig. 1 Chemical formulae of the coupling agents

Table 1 Formulation of the composites

Sample	Wood (%)	PE (%)	TPW 709 (%)	12HSA (%)	MAPE (%)	Si69 (%)	VTMS (%)
Untreated WPC	50	43	3.5	3.5	0	0	0
MAPE treated WPC	50	40	3.5	3.5	3	0	0
Si69 treated WPC	50	40	3.5	3.5	0	3	0
VTMS treated WPC	50	40	3.5	3.5	0	0	3

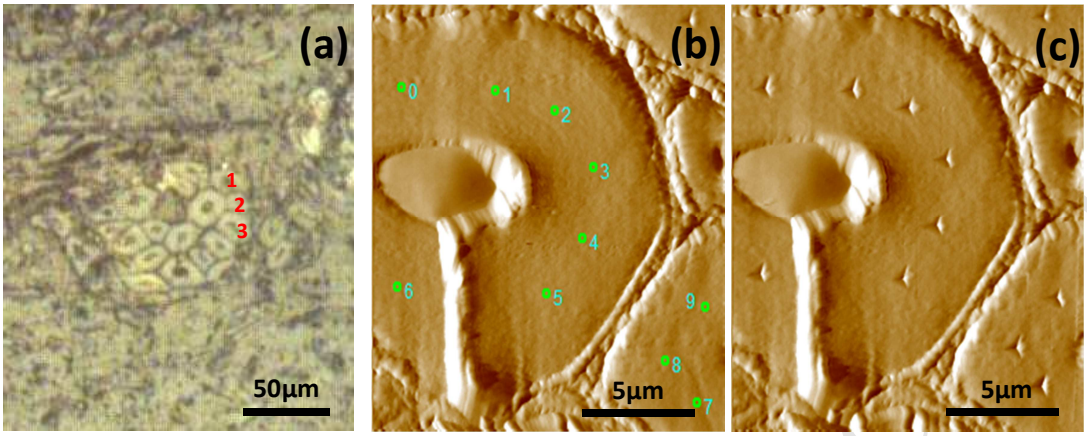

Fig. 2. Typical *in situ* imaging nanoindentation test: (a) microscope image of tested cells in transverse section; (b) image of cell walls in region 1 of Fig.2a before indenting; (c) image of cell walls in region 1 of Fig.2a after indenting.

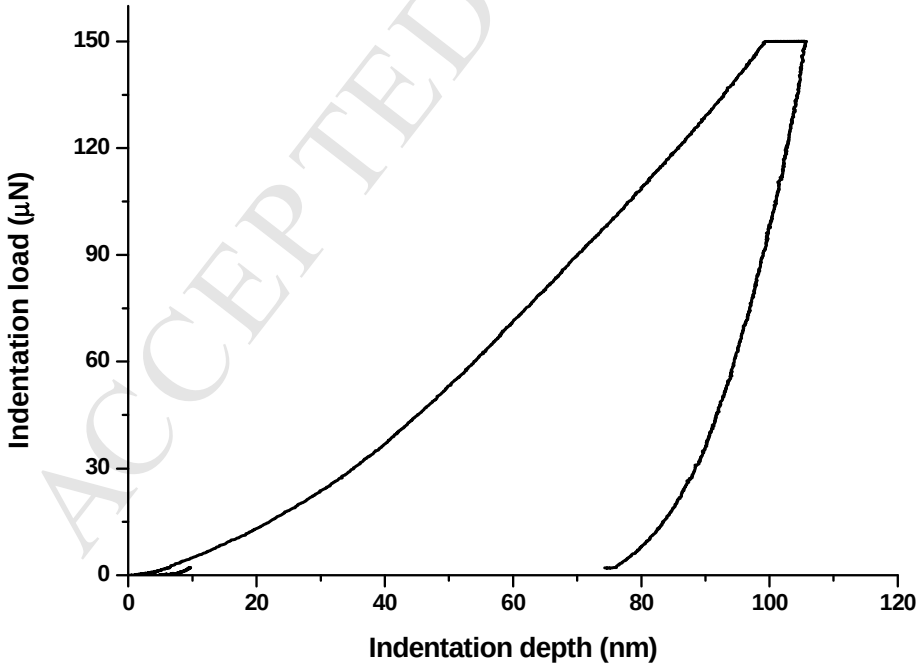

Fig. 3. Typical loading-unloading curve of nanoindentation test

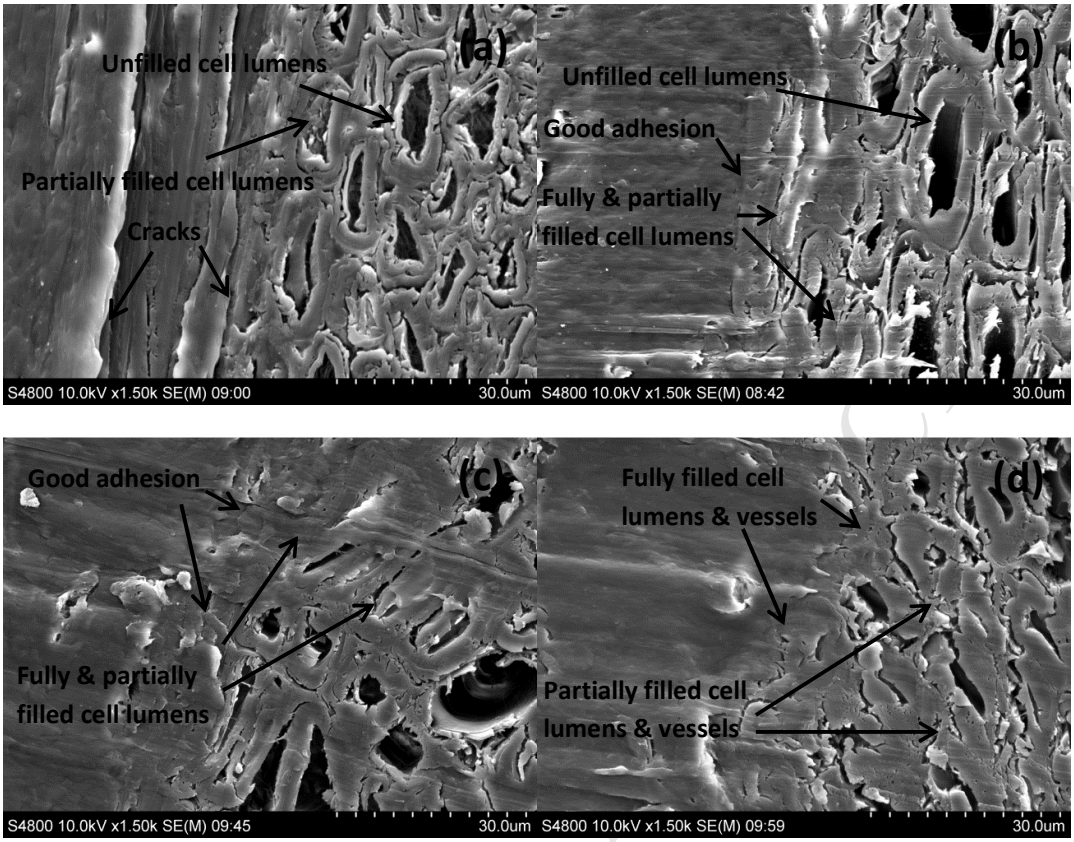

Fig. 4. SEM photographs of cross section of untreated (a), MAPE treated (b), Si69 treated (c) and VTMS treated (d) composites

Table 2 Tensile property of the composites

Sample	**Tensile stress at maximum load (MPa)**	**Tensile strain at maximum load (%)**	**Tensile modulus (MPa)**
Untreated WPC	5.31±0.23	2.36±0.19	1988.75±115.46
MAPE treated WPC	12.50±0.30	1.78±0.16	4230.79±208.73
Si69 treated WPC	6.14±0.25	1.04±0.11	3247.70±170.95
VTMS treated WPC	9.42±0.31	0.96±0.10	4258.92±189.72

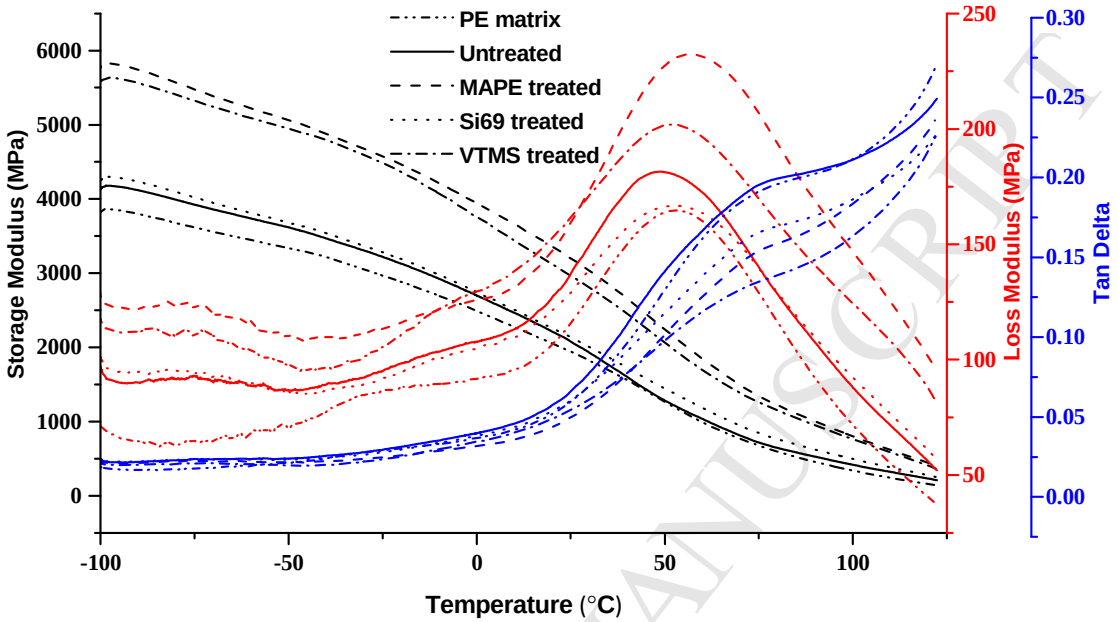

Fig. 5. Storage modulus, loss modulus and tan δ of PE matrix, untreated WPC and treated WPC as a function of temperature

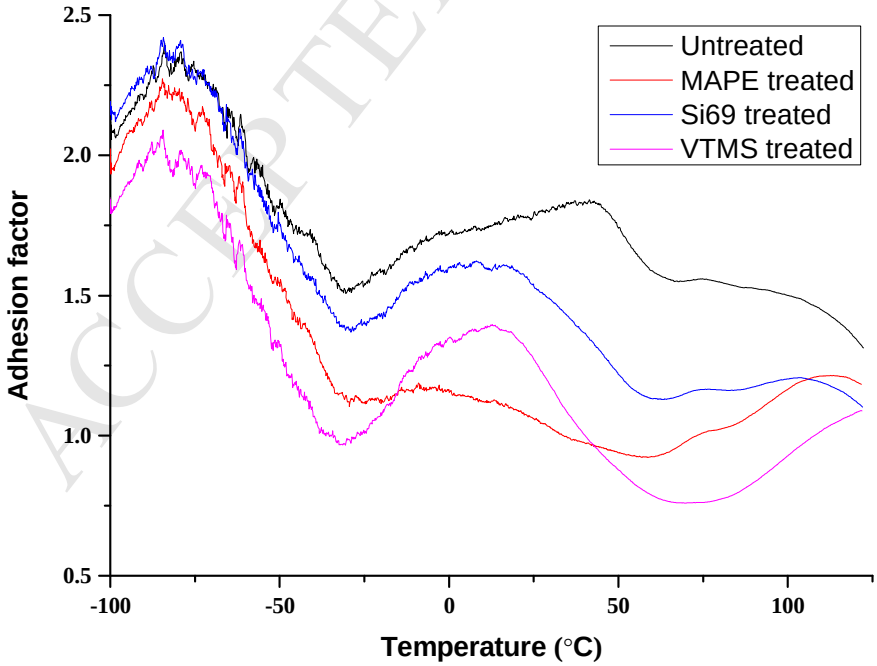

Fig. 6. Adhesion factor of untreated and treated composites as a function of temperature

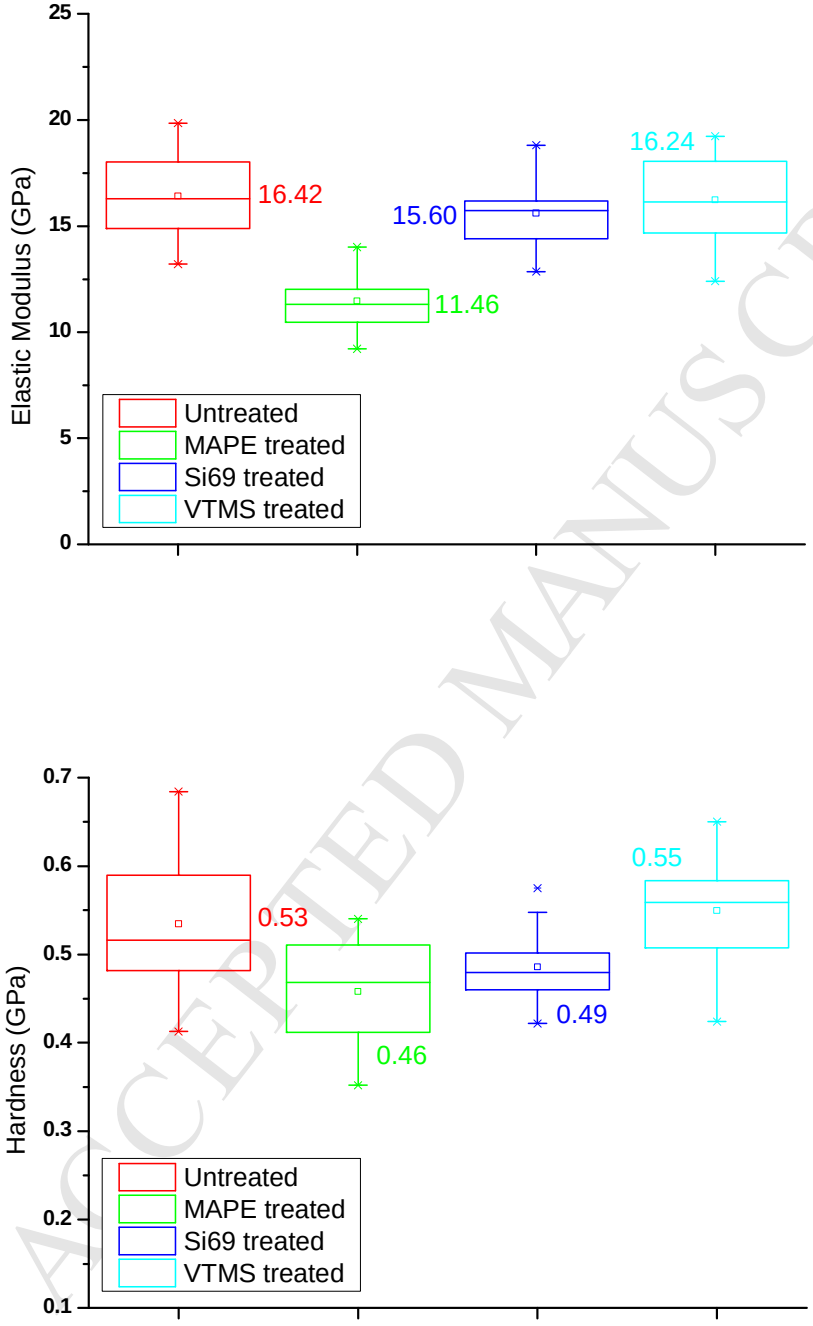

Fig. 7. Nanomechanical property of the composites by nanoindentation